PERGAMON

Planetary and Space Science 48 (2000) 1349–1355

Planetary and Space Science

www.elsevier.nl/locate/planspasci

Windblown dust on Mars: laboratory simulations of flux as a function of surface roughness

Ronald Greeley[a,*], Gregory Wilson[a,1], Rachel Coquilla[b], Bruce White[b], Robert Haberle[c]

[a] *Department of Geology, Arizona State University, Box 871404 Tempe, AZ 85287-1404, USA*
[b] *Department of Mechanical and Aeronautic Engineering, University of California, Davis, CA 95616, USA*
[c] *NASA-Ames Research Center, Mail Stop 245-3, Moffett Field, CA 94035-1000, USA*

Received 9 June 1999; received in revised form 26 January 2000; accepted 27 March 2000

Abstract

Experiments were conducted to determine the flux of dust (particles < few microns in diameter) under Martian atmospheric conditions for surfaces of three aerodynamic roughnesses (z_0). For smooth surfaces on Mars ($z_0 = 0.00125$ cm corresponding to 0.0125 cm on Mars) suspension threshold was not achieved at the highest velocities run ($u_* = 322$ cm/s); for a moderately rough surface ($z_0 = 0.010$ cm corresponding to 0.10 cm on Mars), flux averaged 1.5×10^{-7} g/cm^2/s; for a rough surface ($z_0 = 0.015$ cm corresponding to 0.15 cm on Mars), flux averaged 5×10^{-7} g/cm^2/s. Although the results are preliminary, flux varied widely as a function of wind speed and roughness, suggesting that raising dust into suspension on Mars is complex. Nonetheless, using these results as a guide, 9000 Mt of dust could be raised into the atmosphere of Mars per second from only 5% of the surface. © 2000 Elsevier Science Ltd. All rights reserved.

1. Introduction

Planetary surfaces are shaped or modified by various geologic processes, including volcanism, tectonism, and impact cratering. Terrestrial planets that have dynamic atmospheres are further modified by agents of weathering, erosion, transportation, and deposition. Aeolian, or wind, processes are capable of redistributing enormous quantities of sediment over planetary surfaces, resulting in the formation of landforms large enough to be seen from orbit and deposition of windblown sediments that can be hundreds of meters thick and cover thousands of square kilometers.

Aeolian processes have long been suspected to occur on Mars, based on telescopic observations of shifting color and albedo patterns (see reviews by Kahn et al., 1992; Zurek et al., 1992). Confirmation of aeolian processes came with the Mariner 9 mission in the early 1970s. The Viking mission (1976–1981) provided more detailed information on Martian aeolian features and processes, leading to the analyses of wind erosional features such as yardangs, and study of features for comparison with models of atmospheric circulation (Greeley et al., 1993; Anderson et al., 1999). Reviews of aeolian processes and features on Mars are provided by Wells and Zimbelman (1989), Greeley et al. (1992), Kahn et al. (1992), Zurek et al. (1992), and Zurek and Martin (1993). In addition, Viking infrared thermal inertia mapping (IRTM) data provide information on potential deposits of windblown material (e.g., Christensen, 1986), characteristics of dune deposits (Edgett and Christensen, 1991, 1994), and insight into dust storms (e.g., Peterfreund, 1985; Martin and Richardson, 1993; Martin, 1995). Recent results from the Mars Pathfinder (Golombek et al., 1997; Golombek, 1999) and Mars Global Surveyor missions (Albee et al., 1998; Malin et al., 1998) are providing new insight into the nature of aeolian features and processes seen from the surface (Smith et al., 1997; Greeley et al., 1999) and from orbit (Thomas et al., 1999), respectively.

Most of the information on the nature of small particles (including surface dust) on Mars is derived from Viking Lander data (Moore et al., 1987; Arvidson et al., 1989) and Mars Pathfinder observations (Rover Team, 1997; Smith et al., 1997a). In addition, Viking IRTM data (Kieffer et al., 1977) provide estimates of particle size distributions on the surface of Mars (Christensen and Moore, 1992). Moore and Jakosky (1989) reviewed data for the

* Corresponding author. Tel.: 480-965-7045; fax: 480-965-8102.
E-mail address: greeley@asu.edu (R. Greeley).
[1] Present address: Jet Propulsion Laboratory, 4800 Oak Grove Drive, Pasadena, CA 91109, USA.

0032-0633/00/$ - see front matter © 2000 Elsevier Science Ltd. All rights reserved.
PII: S0032-0633(00)00115-X

Viking landing sites and considered how the results can be extrapolated to other areas using remote sensing data. To summarize these and other observations, "drifts" of material on the surface appear to be composed of fine grains $\leqslant 100$ μm in diameter (Sharp and Malin, 1984) and apply to material on the surface inferred to move in saltation. Particles suspended in the atmosphere (i.e., *dust*) are probably much smaller. Pollack et al. (1995) assessed the atmospheric opacity during both clear periods and during dust storms and estimated that the radius of dust in the atmosphere is on the order of 1.85 μm. More recent analyses of atmospheric dust by Smith et al. (1997), Tomasko et al. (1999), and Markiewicz et al. (1999) using Mars Pathfinder data suggest diameters of a few μm. These small particles are extremely difficult to set into motion by boundary-layer wind-shear alone (Greeley et al., 1980). However, aerodynamic surface roughness influences both the threshold and flux of small particles. Aerodynamic roughness, z_0, is the height above the surface at which the wind velocity is essentially zero (Prandtl, 1935, Bagnold, 1941; Greeley and Iversen, 1985; and others) and is incorporated in the equation

$$u = (u_*/k)\ln(z/z_0), \tag{1}$$

in which u is the wind speed at a given height, u_* the wind friction speed, k the von Karman's constant (0.4), z the height, and z_0 the aerodynamic surface roughness. Aerodynamic surface roughness is a function of many factors, including topography on a scale of meters and the size of the grains on the surface. The influence of various terrains on aerodynamic roughness was demonstrated by Greeley and Iversen (1987). Experiments applied to Mars showed that aerodynamic roughness on the scale of a few cm can lower the wind speeds needed to entrain small particles (White et al., 1997). This is achieved in two ways; first, dust that is settled on individual roughness elements, such as small pebbles, is higher in the boundary layer where the wind shear is stronger than over a smooth surface and, second, turbulence generated around individual rocks creates scour zones where dust is locally entrained. As a follow-on to the dust threshold experiments using rough surfaces, we have investigated the *flux*, or the amount of dust set into suspension under Martian conditions as a function of surface roughness. The initial results of these experiments are reported here.

2. Laboratory simulations

Experiments were carried out in the Mars Surface Wind Tunnel (MARSWIT) at NASA-Ames Research Center, using surrogate Martian dust emplaced on test beds of three surface roughnesses. The flux of dust raised into the atmosphere was determined as a function of wind speed and aerodynamic surface roughness. Flux was quantified as mass removed per unit surface area of the test bed per time (gm/cm^2/s).

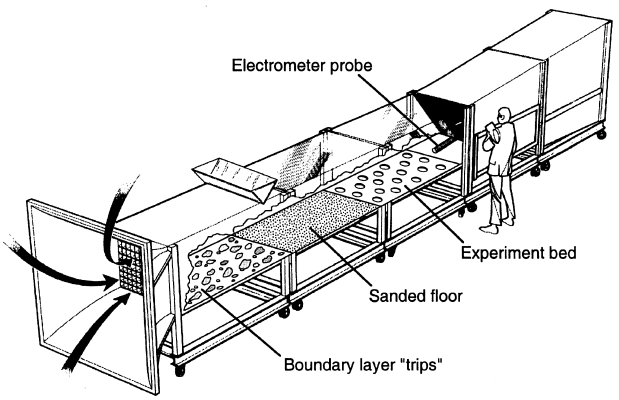

Fig. 1. "Cut-away" diagram of MARSWIT, showing the configuration of the test section with the boundary layer "trips", the sanded floor, and the experiment test bed with the sample disks. Also shown is the electrometer probe used to determine when particles were in motion.

2.1. Wind tunnel

MARSWIT is an open-circuit boundary-layer wind tunnel which is housed inside a 4000 m^3 low-pressure chamber (Greeley et al., 1981). The tunnel has a total length of 13 m and its main test section is 1.2×0.9 m high (Fig. 1). Low atmospheric pressure is achieved by a five-stage steam ejection plant, which enables the chamber to be evacuated to as low as 3.5 mb using either air or carbon dioxide atmospheric composition. At ambient laboratory temperatures, "Earth" air at 10 mb pressure has about the same fluid density as carbon dioxide at ~ 6.5 mb, the nominal case for Mars. Consequently, MARSWIT is typically run using air at 10 mb for Martian simulations.

At Earth standard atmosphere ("one atmosphere"), winds are drawn through the test section using a motor-driven fan at the exit end of the tunnel. At low pressures, winds are generated using a high-pressure air (or CO_2) injection system at the exit end of the tunnel which creates a suction through the tunnel. Using the fan system at Earth standard pressure, freestream (i.e., above the boundary layer) winds (U_∞) through the test section maximize at $\sim 10^3$ cm/s; at 3.5 mb pressures for Mars, freestream velocities as high as 10^4 cm/s are reached.

To conduct the flux experiments, an appropriate medium was required to simulate Martian dust in size and shape, as well as be available and inexpensive. From previous experiments (Greeley et al., 1994, White et al., 1997) a commercially available kaolinitic clay was found to meet these requirements. Termed *Carbondale Red Clay* (CRC), it has a 1.5 μm mean particle diameter, a 2.5 g/cm^3 density, and is available from industrial ceramics suppliers.

To determine the mass lost in the experiments, 24 sample disks, each 10 cm in diameter (0.0079 m^2) and spaced

14 cm apart, were set in the test section floor (Fig. 1). After emplacement of CRC dust, each disk was weighed before and after the test runs. In experiments involving rough surfaces, the masses of roughness elements (pebbles) glued to the disks were included in the weights. The disks were removed and replaced into the test bed using a rotating cam mechanism which enabled movement without disturbing the rest of the test bed. During the experiments, a Keithley Instruments Electrometer Model 600B probe was placed at the end of the wind tunnel test section to determine the time during which dust was removed from the bed. The electrometer measured the electrical charges generated by the impact of wind-blown dust particles. By monitoring the electrometer the operator can determine the time when particles begin to move and when motion ceases.

Atmospheric boundary layer tunnels, such as MARSWIT, require either a long "fetch" between the entrance and the test section in order to obtain a fully developed turbulent boundary layer, or a mechanism to "trip" the flow in order to generate a steady boundary layer. Because of the confined space in the low-pressure chamber and the resulting length of MARSWIT, boundary layer "trips" were placed at the entrance to produce a turbulent zone through the test section (Fig. 1). The "trips" consisted of sets of different size chains and rocks mounted on the floor of the test section. This was followed (downwind) by a section of the floor on which a thin layer of sand grains (350 μm diameter) was glued using a non-outgassing epoxy (Hysol 9309). This surface was then followed by the experiment bed of the test section, which contained the sample disks. CRC was glued to the base of the experiment bed to provide the same type of surface as the test particles. This configuration ("trip" zone, sanded surface, then CRC dust surface) produced a uniform turbulent boundary layer across the experiment beds. The uniformity of the boundary layer was assessed by obtaining wind velocity profiles as a function of height above the test bed for a variety of conditions.

Three roughnesses were tested in these experiments: Case 1 (smooth) consisted of the CRC surface without rocks, Case 2 (moderately rough) involved alternating rows of 1–2 cm in diameter pebbles glued to the floor (including the sampling disks) with a surface density of 255 pebbles/m^2; and Case 3 (rough) in which pebbles were glued to the floor (including the sampling disks) in a density of 510 pebbles/m^2.

2.2. Dust emplacement

In order to deposit particles from atmospheric suspension without imposing artifacts, a method of aerodynamic settling was used so that CRC dust is applied uniformly over the test bed. This was accomplished at Earth standard atmosphere and it involved two 4 l buckets, each containing a 1:5 mixture of CRC dust and sand particles. The buckets were covered with a fine mesh screen and placed at the entrance of the tunnel. Compressed air was then injected into the buckets, during which the larger sand particles loosened the dust from interparticle cohesion, setting the dust into motion for diffusion through the screen (Fig. 2). The sand grains were blocked by the screen and remained in the container. The suspended dust was then carried through the wind tunnel by extremely low speed winds and allowed to settle over the test bed. After about 4–5 h, most of the dust was expelled from the buckets. Dust settling took as long as 12 h and eventually formed a layer of dust over the wind tunnel test section.

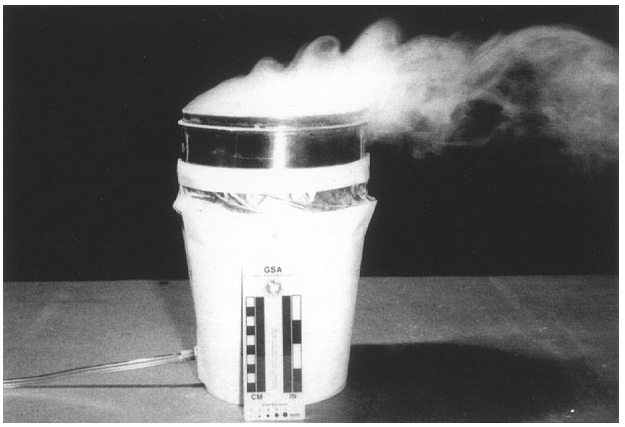

Fig. 2. Simulated Mars dust was entrained in the atmosphere using the technique shown here. A mixture of sand and dust was placed in the bucket which was covered with a fine screen. Air was injected into the mixture through a hose in the side of the bucket (left side in picture), setting the mixture into motion. The screen prevented the escape of the sand, but enabled the passage of the dust (the "smoke" drifting toward the right) into the air above the bucket where it was caught by a gentle wind in the tunnel, causing it to drift over the test section where it settled from suspension onto the test bed.

2.3. Data acquisition

Principal wind tunnel parameters monitored during the experiments were atmospheric temperature, pressure, density, freestream wind velocity (U_∞), and electrometer probe measurements. These were recorded using a data acquisition system (LabVIEW) which provided sampling rates up to 400 Hz, depending on the duration and the number of channels sampled during an experimental run. The advantage of this system is that it provided a near real-time view of critical wind tunnel conditions.

Wind velocity profiles through the boundary layer were required to determine the friction velocity (u_*) exerted by the wind on the surface. Profiles were acquired over the three test-bed roughnesses both before dust was emplaced and during dust-flux runs. The "no dust" profiles were obtained to verify whether a fully developed boundary layer passed over the test beds. They were also used to

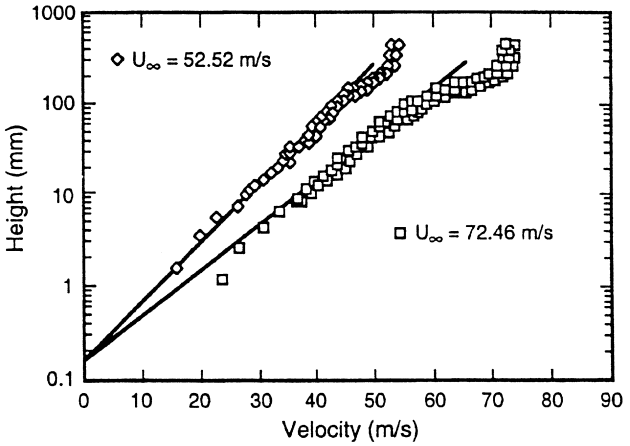

Fig. 3. Typical wind velocity profiles obtained in MARSWIT, showing profiles for Case 3 (rough floor) for two freestream (U_∞) wind speeds at 10 mb atmospheric pressure; lines define the turbulent boundary layer and the intercept gives the z_0 value (for Case 3, $z_0 = 0.015$ cm); the upturn in the data at the higher velocities indicate the freestream flow through the tunnel.

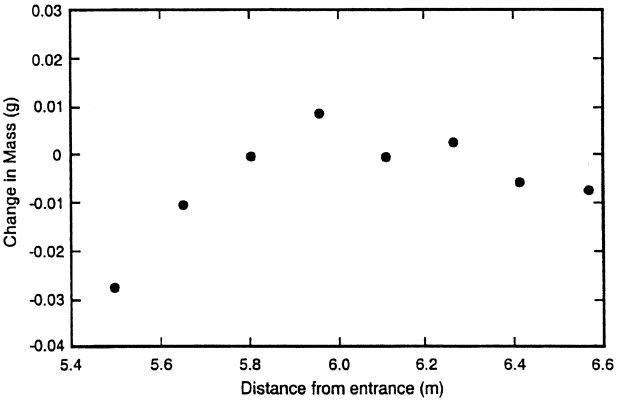

Fig. 4. Mass loss or gain for sample disks as a function of distance from the entrance to the wind tunnel for Case 1 (smooth floor; experiment 008) run at a friction velocity of 273 cm/s. Although there is net loss, dust did not pass into suspension (indicated by lack of response by the electrometer probe); rather, dust accumulated into small clods which tended to roll along the surface, indicated by the mass gain on some of the sample disks.

determine the aerodynamic surface roughnesses over the experiment test beds (Fig. 3).

The turbulent region above the viscous sublayer is described by the logarithmic law of the wall equation (e.g., Prandtl, 1935; Bagnold, 1941):

$$\frac{u}{u_*} = 5.5 \log \frac{u_* z}{v} + 5.45 \quad (2)$$

in which v is the kinematic viscosity. The friction velocity is

$$u_* = U_\infty \sqrt{C_f/2}, \quad (3)$$

in which U_∞ is the freestream wind velocity and C_f is the coefficient of friction. Eq. (1) can be redefined so that the velocity profile is represented by a graph of the non-dimensional local velocity, u/U_∞, versus the log of the local Reynolds number, $U_\infty z/v$. When plotted in comparison with lines of constant skin friction coefficient (C_f), the C_f for the experimental run can then be estimated which will, in turn, enable the derivation of the friction velocity, u_*, using Eq. (3). Profiles of the wind velocities were obtained for a range of freestream velocities in order to characterize the surface roughness and the flow through the wind tunnel. From the wind velocity profiles, we determined that Case 1 (smooth floor) had an aerodynamic roughness of 0.00125 cm, Case 2 (moderately rough floor) was 0.010 cm, and Case 3 (rough floor) was 0.015 cm. Previous experiments by Sullivan and Greeley (1993) show that wind tunnel aerodynamic roughnesses can be scaled to field conditions nearly linearly for modeled roughness elements of 1:10 scales. Based on their results, the aerodynamic roughnesses in the experiments reported here would be increased by an order or magnitude, assuming that the roughness elements (the 1–2 cm pebbles) were modeling rocks 10–20 cm on Mars. Note, however, that this scaling applies only to the nature of the boundary layer and the resulting aerodynamic roughess in MARSWIT compared to Mars. The fluxes of dust raised into the atmosphere from the experiments do not scale by a factor of 10, but are taken to be 1:1 for MARSWIT: Mars because the dust used in the experiments is the same size as estimated for Mars.

3. Results

In observing the behaviour of the dust on the various test beds in preliminary tests, we found that the movement of the dust was not uniform. Some parts of the bed were more active than other parts of the bed. This led to the design in which sample disks were emplaced within the entire experiment test bed. For each experiment run, the mass loss or mass gain of each of the 24 sample disks (including the pebbles in Cases 2 and 3) was measured in order to estimate the total change in mass for the test bed as a whole.

In Case 1 (smooth floor), dust suspension did not occur, even for the high-wind speeds at low pressure ($U_\infty > 3 \times 10^3$ cm/s). Rather, the dust tended to clump into clods which rolled along the test bed and exited the test section. As shown in Fig. 4, some sample disks lost mass, while others gained mass. Although the experiment bed as a whole lost mass, this does not represent a suspension flux. Rather it is the mass of material removed primarily by surface creep and rolling of clumps. The average flux for all Case 1 runs was $\sim 10^{-7}$ g/cm^2/s. We suspect that the clumping results from various electrostatic charges that form in the presence of winds, particularly under Martian conditions, as noted previously (Greeley, 1979) and inferred from the Mars Pathfinder Sojourner results (Ferguson et al., 1999).

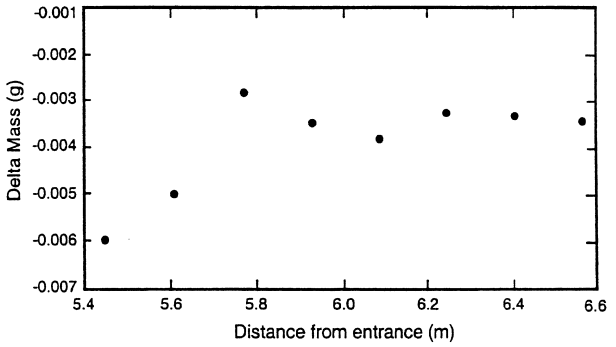

Fig. 5. Mass loss for sample disks as a function of distance from the entrance to the wind tunnel for Case 2 (moderately rough; experiment 015) run at a friction velocity of 353 cm/s, showing general loss of mass over the test floor.

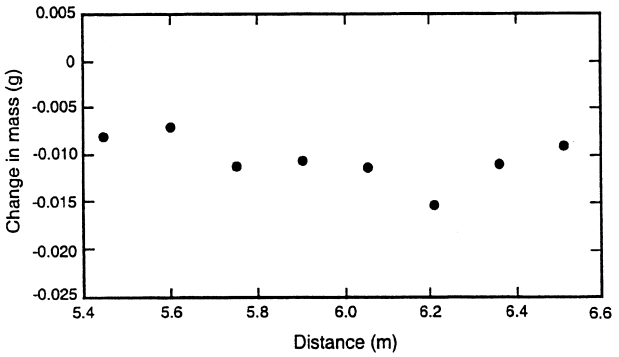

Fig. 6. Mass loss or gain for sample disks as a function of distance from the entrance to the wind tunnel for Case 3 (rough floor; experiment 019).

In Case 2 (moderately rough surface), intermittent threshold of dust occurred at a friction speed of 168 cm/s. The speed was then increased to 353 cm/s and most of the dust was removed from the tops of the pebbles (Fig. 5), but the dust on the bed between the pebbles was not set into motion. The resulting flux averaged 1.5×10^{-7} g/cm^2/s until the tops of the pebbles were cleared, after which the motion ceased and the test bed stabilized. This is considered a non-continuous flux.

Case 3 (rough surface), threshold was achieved at 350 cm/s, with dust being removed not only from the tops of the pebbles, but also from the intervening surfaces of the test bed (Fig. 6). The flux averaged 5×10^{-7} g/cm^2/s, or about three times that of the moderately rough surface.

In general, there was a tendency for flux to increase with freestream velocity for any given roughness, as one might expect (Fig. 7). However, examination of the fluxes as a function of the friction velocities for all three roughnesses reveals a great deal of scatter (Fig. 8). Fig. 9 shows the same data for flux plotted as a function of dimensionless velocity (friction velocity/freestream velocity).

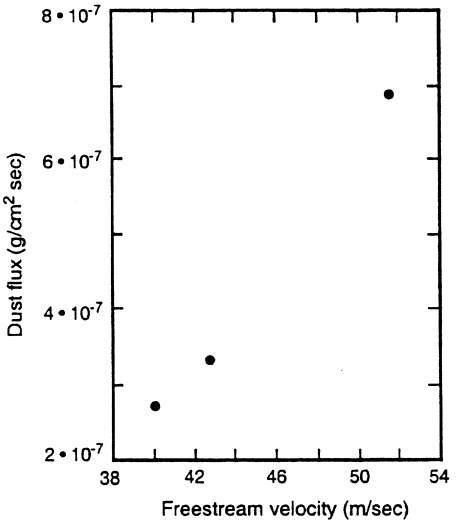

Fig. 7. Average suspended dust flux as a function of freestream velocity (U_∞) for Case 2 (moderately rough).

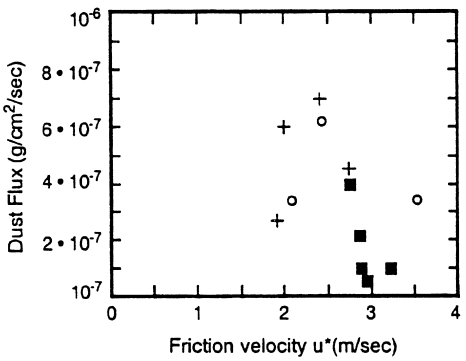

Fig. 8. Suspended dust flux as a function of all three roughness cases; note, however, that Case 1 (smooth) flux is not suspension flux, but reflects material removal by surface creep (squares = smooth; crosses = moderately rough; open circles = rough).

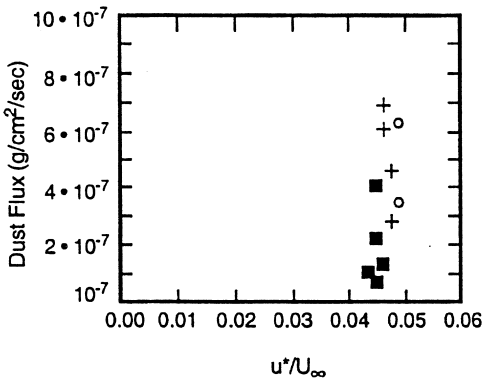

Fig. 9. Suspended dust flux as a function of dimensionless velocity (friction velocity/freestream velocity) (squares = smooth; crosses = moderately rough; open circles = rough).

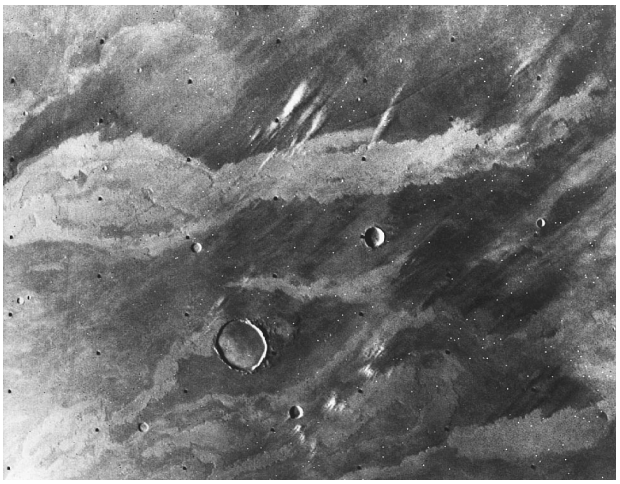

Fig. 10. Dust plumes (bright linear streaks toward bottom of image) rising from lava flow surfaces in the region (23°S, 117°W) southeast of Arsia Mons. Winds are inferred to have been blowing from the north (top of image). Large crater is about 20 km across. (Viking Orbiter image 56A24; Mars $L_s = 109°$; from Briggs et al., 1977).

4. Conclusions

Although the experiments reported here are limited, initial conclusions suggest that flux of suspended dust under Martian conditions is complex, in which both wind speeds and surface roughness are critical factors. What are the implications of the experiment results for Mars? The experiments suggest that it might be very difficult for dust to be raised into suspension on Mars from very smooth surfaces, such as flat plains or former lake beds, unless some sort of roughness elements are present, and that we might expect dust to be more easily raised from surfaces consisting of scattered rocks or other roughness elements. For example, Viking Orbiter images show dust plumes rising from lava flow surfaces in the Arsia Mons region (Briggs et al., 1977), as shown in Fig. 10. Dust settled onto the tops of roughness elements (the lava flow surface) might be more easily raised into suspension than from smoother surfaces.

From the flux measurements obtained here, if we apply a value of 1.3×10^{-7} g/cm^2/s to Mars (a value typical of the experiments involving a pebble bed), then 9000 M t of dust per second could be raised into the atmosphere from only 5% of the Martian surface. Thus, it might not be difficult to account for the frequency and magnitude of Martian dust storms if such a small part of the planet can lead to massive fluxes of dust into the atmosphere. Moreover, the efficiency of dust devils is not taken into account in these estimates, and this mechanism could potentially place even more material into the atmosphere. This value can be compared with the onset of global dust storms on Mars. For example, Martin (1995) estimated that the second Viking global dust storm in 1977 involved 4.3×10^{14} M t of dust in the atmosphere. At 9000 t of dust-raising per second, less than one day would be required to generate this amount of dust suspended in the atmosphere.

An additional consideration is the duration of dust raising. As noted in Case 2, once the dust cleared from the tops of the roughness elements, dust flux ceased and the surface stabilized. Similarly, dust on Mars is likely to be cycling through stages of entrainment, transportation, deposition, and re-entrainment, all involving some steady-state total mass. As outlined previously (Greeley et al., 1992), there are currently relatively few "sinks" (such as oceans) for dust and the production of "new" dust is probably limited. Thus, Martian dust storms might involve the same material that is being recycled repeatedly.

Future experiments will continue to assess the role of roughness in dust flux, with the goal of determining the roughness at which threshold and flux are retarded, rather than enhanced. In principle, once the roughness becomes too great, flux should cease. Additional experiments are planned to assess the efficiency of vortexes ("dust devils") in the threshold and flux of windblown particles on Mars.

Acknowledgements

We thank Rod Leach for identifying the surrogate Mars dust used in these experiments and for developing the techniques to emplace the dust over the test bed. Clay Bratton is thanked for running one of the later experiments in the series described here. We appreciate two anonymous reviewers whose comments significantly improved the manuscript. Sue Selkirk is thanked for providing graphics support. This work was supported by the NASA Planetary Geology and Geophysics Program.

References

Albee, A.L., Palluconi, F.D., Arvidson, R.E., 1998. Mars global surveyor mission: overview and status. Science 279, 1671–1672.

Anderson, F.S., Greeley, R., Xu, P., Lo, E., Blumberg, D.G., Haberle, R.M., Murphy, J.R., 1999. Assessing the Martian surface distribution of aeolian sand using a Mars general circulation model. J. Geophys. Res. Planets, 104, 18,991–19,002.

Arvidson, R.E., Gooding, J.L., Moore, H.J., 1989. The Martian surface as imaged, sampled, and analyzed by the Viking landers. Rev. Geophys. 27, 39–60.

Bagnold, R.A., 1941. The Physics of Blown Sand and Desert Dunes. Methuen, London, 241 pp.

Briggs, G., Klaasen, K., Thorpe, T., Wellman, J., Baum, W., 1977. Martian dynamical phenomena during June–November 1976; Viking Orbiter imaging results. J. Geophys. Res. 82, 4121–4149.

Christensen, P.R., 1986. Regional dust deposits on Mars: physical properties, age, and history. J. Geophys. Res. 91, 3533–3545.

Christensen, P.R., Moore, H., 1992. The Martian surface layer. In: Kieffer, H.H., et al. (Ed.), Mars. University of Arizona Press, Tucson, pp. 686–729.

Edgett, K.S., Christensen, P.R., 1991. The particle size of Martian aeolian dunes. J. Geophys. Res. 96, 22,765–22,776.

Edgett, K.S., Christensen, P.R., 1994. Mars aeolian sand: regional variations among dark-hued crater floor features. J. Geophys. Res. 99, 1997–2018.

Ferguson, D.C., Kolecki, J.C., Siebert, M.W., Wilt, D.M., Matijevic, J.B., 1999. Evidence for Martian electrostatic charging and abrasive wheel wear from the Wheel Abrasion Experiment on the Pathfinder Sojourner rover. J. Geophys. Res. 104, 8747–8789.

Golombek, M.P., Cook, R.A., Economou, T., Folkner, W.M., Haldemann, A.F.C., Kallemeyn, P.H., Knudsen, J.M., Manning, R.M., Moore, H.J., Parker, T.J., Rieder, R., Schofield, J.T., Smith, P.H., Vaughan, R.M., 1997. Over view of the Mars Pathfinder mission and assessment of landing site predictions. Science 278, 1743–1748.

Golombek, M.P., 1999. The Mars Pathfinder Science Team, Overview of the Mars Pathfinder Mission: launch through landing, surface operations, data sets, and Science results (Special Mars Pathfinder issue). J. Geophys. Res. 104, 8523–8554.

Greeley, R., 1979. Silt clay aggregates on Mars. J. Geophys, Res. 84, 6248–6254.

Greeley, R., Iversen, J.D., 1985. Wind as a Geological Process. Cambridge University Press, Cambridge, 333 pp.

Greeley, R., Iversen, J.D., 1987. Measurements of wind friction speeds over lava surfaces and assessment of sediment transport. Geophys. Res. Lett. 14, 925–928.

Greeley, R., Leach, R., White, B., Iversen, J., Pollack, J., 1980. Threshold windspeeds for sand on Mars: wind tunnel simulations. Geophys. Res. Lett. 7, 121–124.

Greeley, R., White, B.R., Pollack, J.B., Iversen, J.D., Leach, R.N., 1981. Dust storms on Mars: considerations and simulations. Geol. Soc. Am. (Special Paper) 186, 101–121.

Greeley, R., Lancaster, N., Lee, S., Thomas, P., 1992. Martian aeolian processes, sediments, and features. In: Kieffer, H.H., et al. (Ed.), Mars. University of Arizona Press, Tucson, pp. 730–766.

Greeley, R., Skypeck, A., Pollack, J.B., 1993. Martian aeolian features and deposits: comparisons with general circulation model results. J. Geophys. Res. 98, 3183–3196.

Greeley, R., Lacchia, M., White, B., Leach, R., Trilling, D., Pollack, J., 1994. Dust on Mars: new values for wind threshold. Lunar Planet Science Conference, Vol. 25, pp. 467–468.

Greeley, R., Kraft, M., Sullivan, R., Wilson, G., Bridges, N., Herkenhoff, K., Kuzmin, R.O., Malin, M., Ward, W., 1999. Aeolian features and processes at the Mars Pathfinder landing site (Special Mars Pathfinder Issue). J. Geophys. Res. 104, 8573–8584.

Kahn, R.A., Martin, T.Z., Zurek, R.W., Lee, S.W., 1992. The Martian dust cycle. In: Kieffer, H.H., et al. (Ed.), Mars. University of Arizona Press, Tucson, pp. 1017–1053.

Kieffer, H.H., Martin, T.Z., Peterfreund, A.R., Jakosky, B.M., Miner, E.D., Palluconi, F.D., 1977. Thermal and albedo mapping of the Mars during the Viking primary mission. J. Geophys. Res. 82, 4249–4291.

Malin, M.C., et al., 1998. Early views of the Martian surface from the Mars Orbiter Camera of Mars Global Surveyor. Science 279, 1681–1685.

Markiewicz, W.J., Sablotny, R.M., Keller, H.U., Thomas, N., Titov, D., Smith, P.H., 1999. Optical properties of the Martian aerosols as derived from Imager for Mars Pathfinder midday sky brightness data. J. Geophys. Res. 104, 9009–9017.

Martin, T.Z., 1995. Mass of dust in the Martian atmosphere. J. Geophys. Res. 100, 7509–7512.

Martin, T.Z., Richardson, M.I., 1993. New dust opacity mapping from Viking Infrared Thermal Mapper data. J. Geophys. Res. 98, 10,941–10,949.

Moore, H.J., Jakosky, B.M., 1989. Viking landing sites, remote sensing observations, and physical properties of Martian surface materials. Icarus 81, 164–184.

Moore, H.J., Hutton, R.E., Clow, G.D., Spitzer, C.R., 1987. Physical properties of the surface materials of the Viking landing sites on Mars. U.S. Geological Survey of Professional Papers, No. 1389, 222 pp.

Peterfreund, A.R., 1985. Contemporary aeolian process on Mars: local dust storms. Ph.D. Dissertation, Arizona State University, Tempe.

Pollack, J.B., Ockert-Bell, M.E., Shepard, M.K., 1995. Viking lander image analysis of Martian atmospheric dust. J. Geophys. Res. 100, 5235–5250.

Prandtl, L., 1935. The mechanics of viscous fluids. In: Durand, F. (Ed.), Aerodynamic Theory, Vol. III. Julius. Springer, Berlin, pp. 57–109.

Rover Team, 1997. Characterization of the Martian surface deposits by the Mars Pathfinder Rover, Sojourner. Science 278, 1765–1768.

Sharp, R.P., Malin, M.C., 1984. Surface geology from Viking landers on Mars: a second look. Geol. Soc. Amer. Bull. 96, 1398–1412.

Smith, P.H., Bell III, J.F., Bridges, N.T., Britt, D.T., Gaddis, L., Greeley, R., Keller, H.U., Herkenhoff, K.E., Jaumann, R., Johnson, J.R., Kirk, R.L., Lemmon, M., Maki, J.N., Malin, M.C., Murchie, S.L., Oberst, J., Parker, T.J., Reid, R.J., Sablotny, R., Soderblom, L.A., Stoker, C., Sullivan, R., Thomas, N., Tomasko, M.G., Ward, W., Wegryn, E., 1997. Results from the Mars Pathfinder Camera. Science 278, 1758–1765.

Sullivan, R., Greeley, R., 1993. Comparison of aerodynamic roughness measured in a field experiment and in a wind tunnel simulation. J. Wind Engng. Ind. Aerodyn. 48, 25–50.

Thomas, P.C., et al., 1999. Bright dunes on Mars. Nature 397, 592–594.

Tomasko, M.G., Doose, L.R., Lemmon, M., Smith, P.H., Wegryn, E., 1999. Properties of dust in the Martian atmosphere from the Imager on Mars Pathfinder. J. Geophys. Res. 104, 8987–9007.

Wells, G.L., Zimbelman, J.R., 1989. Extraterrestrial arid surface processes. In: Thomas, D.S.G. (Ed.), Arid Zone Geomorphology. Belhaven-Halsted, London, pp. 335–358.

White, B.R., Lacchia, B.M., Greeley, R., Leach, R.N., 1997. Aeolian behavior of dust in a simulated Martian environment. J. Geophys. Res. 102, 25,629–25,640.

Zurek, R.W., Barnes, J.R., Haberle, R.M., Pollack, J.B., Tillman, J.E., Leovy, C.B., 1992. Dynamics of the atmosphere of Mars. In: Kieffer, H.H., Jakosky, B.M., Snyder, C.W., Matthews, M.S. (Eds.), Mars. University Arizona Press, Tucson, pp. 835–933.

Zurek, R.W., Martin, L.J., 1993. Inter annual variability of planet-encircling dust storms on Mars. J. Geophys. Res. 98, 3247–3254.